

COMPARISON BETWEEN THEORETICAL AND NUMERICAL SOLUTIONS FOR CENTER, SINGLE EDGE AND DOUBLE EDGE CRACKED FINITE PLATE SUBJECTED TO TENSION STRESS

NAJAH R. MOHSIN

Department of Mechanical Technics, Technical Institute, Southern Technical University, Nasiriya, Iraq

ABSTRACT

The stress intensity factor is one of the most important concepts in fracture mechanics because of stresses near the crack tip increase in proportion to it. Therefore, it must be calculated accurately to obtain the fracture damage. This paper deals with determination of the stress intensity factor mode I (KI) for Centre Cracked Tension (CCT), Single Edge Notch Tension (SENT) and Double Edge Notch Tension (DENT) finite plates under Linear Elastic Fracture Mechanics (LEFM) and plane strain assumptions. To investigate the differences between the theoretical and numerical solutions, a comparison is made between the stress intensity factors calculated using a large number of standard equations with the others calculated using finite element software ANSYS R14.5. Stress intensity factors are evaluated with variation of crack length to plate width ratio (a/b), tensile stresses ($\bar{\sigma}_t$) and plate length to plate width (h/b). The analysis shows that the numerical solution is more suitable than the theoretical solution due to the results that the theoretical equations are limited in a range of parameters values, some parameters such as length plate is not considered in it and also the difficulty to determine the accurate stress intensity factors for cracks in complex structures.

KEYWORDS: Stress Intensity Factor, Centre Cracked Tension (Cct), Single Edge Notch Tension (Sent), Double Edge Notch Tension (Dent), Ansys R14.5

INTRODUCTION

The prediction of the mechanical behavior of a structure when it is subjected to an external load such as tension represents the basic problem in mechanics. In the design, our aim is to predict the deformation and stresses that happen in the material to avoid catastrophic failures occurred. Stresses are concentrated and reached to a large values at the geometry discontinuities as holes, corners, notches, cracks etc .

The fracture mechanics theory can be used to analyze structures and machine components with cracks and to obtain an efficient design. The basic principles of fracture mechanics developed from the studies of Inglis, Griffith and Trans are based on the concepts of linear elasticity. Westergaard derived the general linear elastic solution for the stress field around a crack tip using complex stress functions, Bhagat and et al. [1]. Irwin was one of the first to study the behavior of cracks. He introduced three different loading modes (Figure 1), which are still used today: Mode I = opening mode, Mode II = sliding mode and Mode III = tearing mode, Schreurs[2].

Huang and Kardomateas [3] formulated an approach based on the continuous dislocation technique to obtain the stress intensity factors for mode I and II in a fully anisotropic infinite strip with a central crack. Chin [4] used the finite element software ANSYS and the crack growth software FRANC3D to investigate how a crack propagates and grows in a

typical Ti-6Al-4V aerospace bracket by computing the stresses and the stress-intensity factor. A specific bracket design was selected and a corner crack was investigated. The effect of crack inclination angle on stress intensity factors for two parallel and non parallel cracks using ANSYS software was studied by Bhagat and et al. [1]. Ergun and et al. [5] used the Finite Element Method (FEM) to analyze the behavior of repaired cracks in 2024-T3 aluminum with bonded composite. Stress intensity factors mode I were calculated based on displacement correlation technique. Ali and et al. [6] analyzed the stress intensity factor in various edge cracks along the length of a finite plate which was under a uniform tension using FEM. Al-Ansari [7] calculated a stress intensity factor mode I of unidirectional composite center cracked plate with the effect of volume fraction of unidirectional fiber using FEM.

To predict the behavior of a crack, it is essential to know its location, geometry and dimensions. In this paper attention is given to calculate the stress intensity factor for center, single edge notch and double edge notch cracked finite plates. Throughout this paper, it is assumed that the material behavior is linear elastic and isotropic.

MATERIALS AND METHODS

Finite-width plate specimens with Centre Cracked Tension (CCT), Single Edge Notch Tension (SENT) and Double Edge Notch Tension (DENT) subjected to uniform uni-axial tension stresses in the Y- direction as shown in Figure 2 are studied to determine the stress intensity factors mode I (KI) using numerical and theoretical solutions under the assumptions of Linear Elastic Fracture Mechanics (LEFM) and plane strain.

Specimens Material

The material of plates is carbon steel with modulus of elasticity = $202 \times 10^3 \text{ MN/m}^2$ and poisson's ratio = 0.292.

Theoretical Solution

Previously, a large number of equations were formulated to calculate approximately the stress intensity factors. In this paper, five different theoretical equations from different references are selected to calculate the stress intensity factors for each type of the three plate specimens as shown in the Table 1.

Numerical Solution

Stress intensity factors are calculated numerically using finite element software ANSYS R14.5 with PLANE183 element as a discretization element. As a reason of symmetry, half model is used in SENT case and quarter models are used in case of CCT and DENT as shown in Figure 2. CCT, SENT and DENT ANSYS models are shown in Figure 3 with the mesh, elements, nodes and boundary conditions.

PLANE183 Description

PLANE183 = element type is defined by 8 nodes (I, J, K, L, M, N, O, P when quadrilateral element) or 6 nodes (I, J, K, L, M, N when triangle element) having two degrees of freedom (UX, UY) at each node (translations in the nodal X and Y directions). It has quadratic displacement behavior and is well suited to modeling irregular meshes. Element loads are described in nodal loading. Pressures may be input as surface loads on the element faces. Positive pressures act into the element and temperatures may be input as element body loads at the nodes, ANSYS help [11]. The geometry, node locations, and the coordinate system for this element are shown in Figure 4. PLANE183 is used in this paper as a discretization element with quadrilateral shape, plane strain behavior and pure displacement formulation.

The Studied Cases

To illustrate the difference between theoretical and numerical solutions for CCT, SENT and DENT the stress intensity factors for many cases are studied theoretically using a large number of equations and numerically using finite element software ANSYS R14.5. The results of all studied cases are reported in Table 2.

RESULTS AND DISCUSSIONS

KI values are theoretically calculated using different equations and numerically using ANSYS R14.5 for three different types of cracked plate specimens (CCT, SENT and DENT) with different cases reported in Table 1.

The Numerical Compression

Case Study I

Figure 5-7 explain the numerical and theoretical variations of stress intensity factors KI with different values of a/b ratio as shown in Table 2. From these figures, it can be seen that increasing the ratio of a/b leads to increasing the value of KI in a high level for all the selected values. These figures also show a fitness between theoretical and numerical solutions at a/b=0.3 for SENT and at a/b<0.25 for CCT and DENT. A small difference occurs between the two solutions at a/b>0.25 for CCT and at a/b>0.3 for SENT while a sensitive difference occurs at a/b>0.25 for DENT.

Case Study II

Figure 8-10 show the variation of KI with different values of tension stresses (shown in Table 2). It can be seen from these figures that there are fitness between numerical and theoretical solutions for all plate specimen types (CCT, SENT and DENT) except small difference, (7) and (12) for SENT and DENT, respectively.

Case Study III

Figure 11-13 illustrate the theoretical and numerical variations of KI with different values of h/b ratio as shown in Table 2. From all these figures, we shown that a large difference between numerical and theoretical solution at h/b<1 but this difference will vanish at h/b>1 except of (7) and (12) for SENT and DENT, respectively.

The variation of numerically computed KI for the three of different cracked plate specimens (CCT, SENT and DENT) in I, II and III cases are shown in Figure 14-16, respectively. In all mentioned figures, it is found that the KI values in CCT are less than that of SENT and DENT. From Figure 14 and Figure 15, it is clear that the values of KI for SENT are greater than that from DENT, while from Figure 16 we shown that the values of KI equal at h/b < 0.5 and after then when h/b > 0.5 the values of KI for DENT will be greater than that for SENT.

Furthermore, Figures 17a, b, c, d, e, f graphically illustrated Von-Mises stresses contour plots with deformed shape for the cracked plate specimens for different states. Figures 17a, c, e show the variation of $\sigma_{\text{von-mises}}$ for CCT, SENT and DENT, respectively when b=0.2m, h=0.2m, a=0.03m and $\sigma_t=200\text{Mpa}$. The variation of $\sigma_{\text{von-mises}}$ for CCT, SENT and DENT, respectively when b=0.2m, h=0.2m, a=0.08m and $\sigma_t=100\text{Mpa}$ are shown in Figures 17b, d, f.

CONCLUSIONS

- KI values are calculated from the theoretical equations for different cases are approximately same in all cases except the values calculated from (12) and (15) for the case of DENT, (2) in case of CCT and (7) in case of SENT.

- Numerical solution results coincide with the theoretical solutions for many cases except when $h/b < 1$. At this point, KI is not suitable to calculate using theoretical approach because it doesn't take this parameter in consideration.
- Numerical solution is more suitable to calculate KI due to all theoretical equations are limited for some cases and for regular geometry while the numerical solution is used for all cases and with regular and irregular shapes.

REFERENCES

1. R. K. Bhagat, V. K. Singh, P. C. Gope, A. K. Chaudhary. Evaluation of stress intensity factor of multiple inclined cracks under biaxial loading. *Frattura ed Integrità Strutturale*, Vol.22, pp. 5-11,2012.
2. P. J. G. Schreurs. *Fracture Mechanics*, Lecture notes - course 4A780, Eindhoven University of Technology, Department of Mechanical Engineering, Materials Technology. <http://www.mate.tue.nl/~piet/edu/frm/pdf/frmsyl1213.pdf>,2012.
3. H. Huang and G. A. Kardomateas. Stress intensity factors for a mixed mode center crack in an anisotropic strip. *International Journal of Fracture*, Vol. 108, pp. 367–381, 2001.
4. P. L. Chin. Stress Analysis, Crack Propagation and Stress Intensity Factor Computation of a Ti-6Al-4V Aerospace Bracket using ANSYS and FRANC3D. MSc theses, Rensselaer Polytechnic Institute, Hartford, 2011.
5. E. Ergun, S. Tasgetiren and M. Topcu. Patch by combined genetic algorithms and FEM under temperature effects stress intensity factor estimation of repaired aluminum plate with bonded composite. *Indian Journal of Engineering & Materials Sciences*, Vol. 19, pp. 17-23, 2012.
6. Z. Ali, K. E. S. Meysam, AsadiIman, B. Aydin and B. Yashar. Finite Element Method Analysis of Stress Intensity Factor in Different Edge Crack Positions, and Predicting their Correlation using Neural Network method. *Research Journal of Recent Sciences*, Vol. 3(2), pp. 69-73, 2014.
7. L. S. Al-Ansari. Investigating the effect of Volume Fraction on the Stress Intensity Factor for Composite Plate with Central Crack *International Journal of Mechanical & Mechatronics Engineering*. Vol. 14, PP. 54-64, 2014.
8. H. Tada, P. C. Paris and G. R. Irwin. *The Stress Analysis of Cracks Handbook*. Third edition, ASME press, 2000.
9. A. Fatemi. Fundamentals of LEFM and Applications to Fatigue crack growth -Chapter 6-LEFM & Crack Growth Approach. https://www.efatigue.com/training/Chapter_6.pdf.
10. V. E. Saouma. Lecture Notes in: *FRACTURE MECHANICS-Chapter4*. <http://civil.colorado.edu/~saouma/Lecture-Notes/lecfrac.pdf>.
11. ANSYS help.

APPENDICES

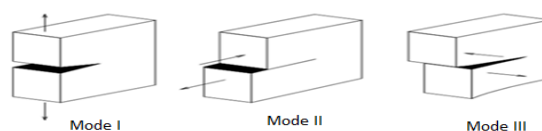


Figure 1: Three Standard Loading Modes of a Crack, Schreurs [2]

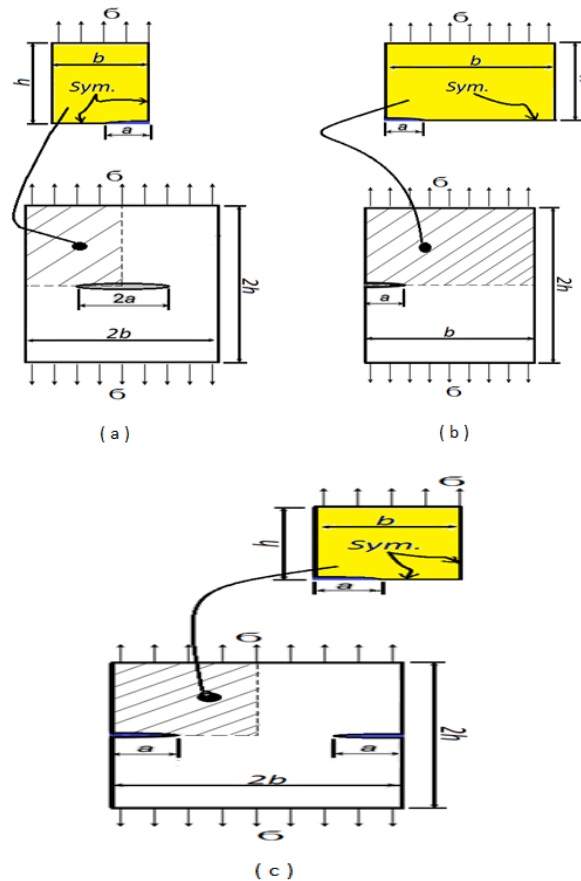


Figure 2: Cracked Plate Specimens with Dimensions for a) CCT b) SENT C) DENT

Table 1: Theoretical Equations that are Used in this Paper to Calculate Stress Intensity Factors K_I

Cracked Plate Type	Eq. Formula	Eq. No.	Ref. No.	conditions
CCT	$K_I = \sigma \sqrt{\pi a} \left[\sqrt{\sec\left(\frac{\pi a}{2b}\right)} \left[1 - 0.025 \left(\frac{a}{b}\right)^2 + 0.06 \left(\frac{a}{b}\right)^4 \right] \right] \dots\dots\dots$	(1)	[8]	----- -
	$K_I = \sigma \sqrt{\pi a} \sqrt{\frac{2b}{\pi a} \tan\left(\frac{\pi a}{2b}\right)} \dots\dots\dots$	(2)	[8]	----- -
	$K_I = \sigma \sqrt{\pi a} \left(1 + 0.128 \left(\frac{a}{b}\right) - 0.288 \left(\frac{a}{b}\right)^2 + 1.525 \left(\frac{a}{b}\right)^3 \right) \dots\dots\dots$	(3)	[8]	(a/b) ≤ 0.5
	$K_I = \sigma \sqrt{\pi a} \sqrt{\sec\left(\frac{\pi a}{b}\right)} \dots\dots\dots$	(4)	[9]	----- -
	$K_I = \sigma * \sqrt{\pi * a} * \left \frac{1 - 0.5\left(\frac{a}{b}\right) + 0.37\left(\frac{a}{b}\right)^2 - 0.044\left(\frac{a}{b}\right)^3}{\sqrt{1 - \frac{a}{b}}} \right \dots\dots\dots$	(5)	[8]	----- -
SENT	$K_I = \sigma \sqrt{\pi a} \left[1.12 - 0.23 \left(\frac{a}{b}\right) + 10.56 \left(\frac{a}{b}\right)^2 - 21.74 \left(\frac{a}{b}\right)^3 + 30.42 \left(\frac{a}{b}\right)^4 \right] \dots\dots\dots$	(6)	[10]	(h/b) = 2
	$K_I = \sigma \sqrt{\pi * a} \left[\frac{\sqrt{\frac{2b}{\pi a} + \tan\frac{\pi a}{2b}}}{\cos\frac{\pi a}{2b}} \right] \left[0.752 + 2.02 \left(\frac{a}{b}\right) + 0.37 \left(1 - \sin\frac{\pi a}{2b}\right)^3 \right] \dots\dots\dots$	(7)	[8]	----- -

	$K_I = \sigma\sqrt{\pi * a} \left[0.265 \left(1 - \frac{a}{b} \right)^4 + \frac{0.857 + 0.265 \frac{a}{b}}{\left(1 - \frac{a}{b} \right)^{\frac{3}{2}}} \right]$	(8)	[8]	$\left(\frac{a}{b} \right) < 0.6$
	$K_I = \sigma\sqrt{a} \left[1.99 - 0.41 \left(\frac{a}{b} \right) + 18.7 \left(\frac{a}{b} \right)^2 - 38.48 \left(\frac{a}{b} \right)^3 + 53.85 \left(\frac{a}{b} \right)^4 \right]$	(9)	[9]	----- -
	$K_I = \sigma\sqrt{a} \left[1.12\sqrt{\pi} - 0.41 \left(\frac{a}{b} \right) + 18.7 \left(\frac{a}{b} \right)^2 - 38.48 \left(\frac{a}{b} \right)^3 + 53.85 \left(\frac{a}{b} \right)^4 \right]$	(10)	[2]	----- -
DENT	$K_I = [1.12 + 0.204 \left(\frac{a}{b} \right) - 1.197 \left(\frac{a}{b} \right)^2 + 1.93 \left(\frac{a}{b} \right)^3] \sigma\sqrt{\pi a}$	(11)	[8]	----- -
	$K_I = \sigma\sqrt{\pi a} \left[\left(1.122 - 0.561 \left(\frac{a}{b} \right) - 0.015 \left(\frac{a}{b} \right)^2 + 0.091 \left(\frac{a}{b} \right)^3 \right) / \left(\sqrt{1 - \left(\frac{a}{b} \right)^2} \right) \right]$	(12)	[8]	$\left(\frac{a}{b} \right) < 0.7$
	$K_I = \sigma\sqrt{\pi a} \left[\left(1.122 - 0.561 \left(\frac{a}{b} \right) - 0.205 \left(\frac{a}{b} \right)^2 + 0.471 \left(\frac{a}{b} \right)^3 \right) - 0.19 \left(\frac{a}{b} \right) \right]$	(13)	[8]	----- -
	$K_I = [1.12 + 0.43 \left(\frac{a}{b} \right) - 4.79 \left(\frac{a}{b} \right)^2 + 15.46 \left(\frac{a}{b} \right)^3] \sigma\sqrt{\pi a}$	(14)	[10]	----- -
	$K_I = \sigma\sqrt{a} \left[1.12\sqrt{\pi} + 0.76 \frac{a}{b} - 8.48 \left(\frac{a}{b} \right)^2 + 27.36 \left(\frac{a}{b} \right)^3 \right]$	(15)	[2]	----- -

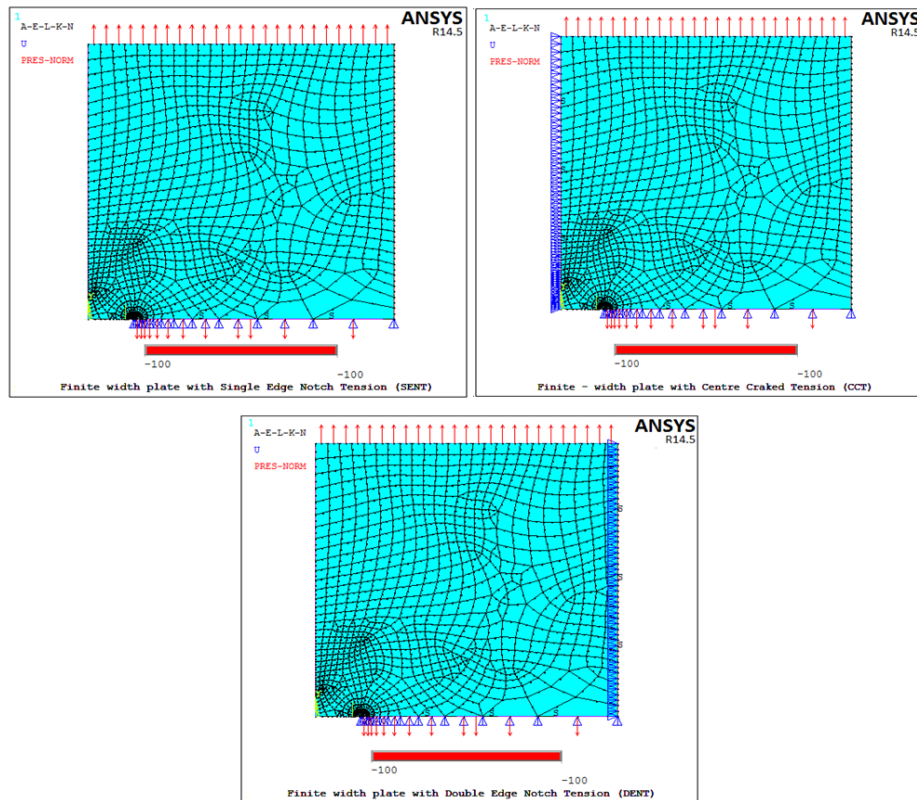


Figure 3: Mesh Generation with 556 Elements, 1709 Nodes and Boundary conditions for a) CCT B) SENT C) DENT

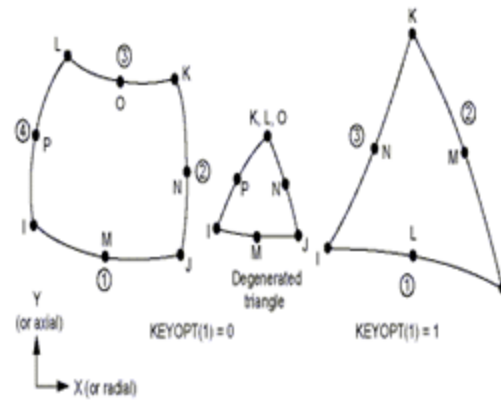


Figure 4: The Geometry, Node locations, and the Coordinate System for Element Plane183, ANSYS Help[11]

Table 2: The Cases Studied with the Plate, Solution Types and Number of Figures

No. of Studied Cases	Changed Parameter in this Case Study		Other Parameters	Numerical & Theoretical Solutions			Numerical Solution Only
	Name	Values (m)		Plate Type & Figure No.			Plate Type & Figure No.
I	a/b	0.02	$\sigma_t = 100$ Mpa b = 0.2 m h = 0.2 m	CCT	SENT	DENT	CCT, SENT& DENT
		0.03					
		0.04					
		0.05					
		0.06					
		0.07					
		0.08					
		0.09					
		0.1					
II	$\sigma_t = 100$ Mpa	50	a = 0.03 m b = 0.2 m h = 0.2 m	CCT	SENT	DENT	CCT, SENT& DENT
		75					
		100					
		125					
		150					
		175					
		200					
		225					
		250					
III	h/b	0.02	a = 0.03 m $\sigma_t = 100$ Mpa b = 0.2 m S	CCT	SENT	DENT	CCT, SENT& DENT
		0.04					
		0.06					
		0.08					
		0.1					
		0.2					
		0.3					
		0.4					

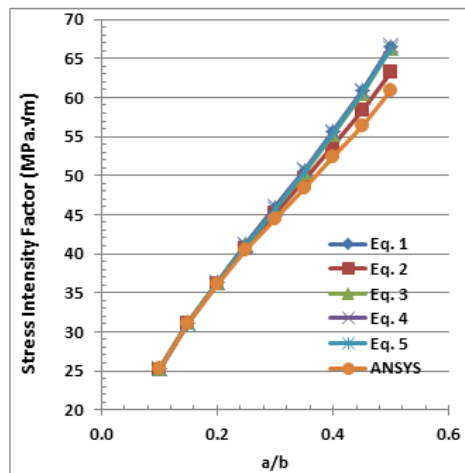


Figure 5: Variation of Stress Intensity Factor with (a/b) Ratio theoretically and Numerically for CCT

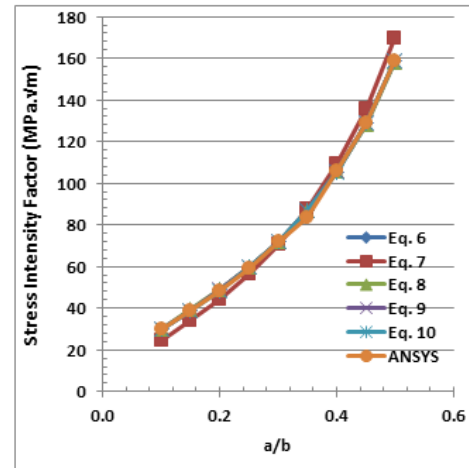


Figure 6: Variation of Stress Intensity Factor with (a/b) Ratio theoretically and numerically for SENT

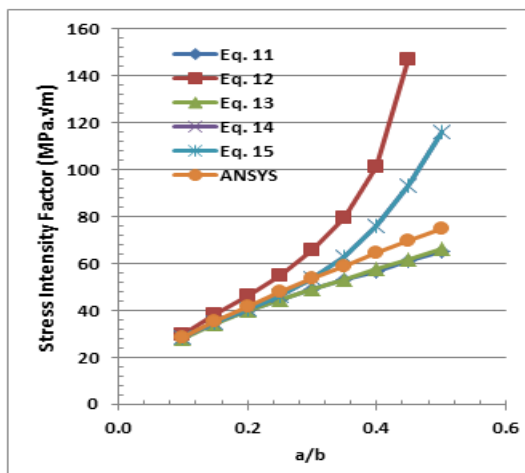


Figure 7: Variation of Stress Intensity Factor with (a/b) Ratio Theoretically and Numerically for DENT

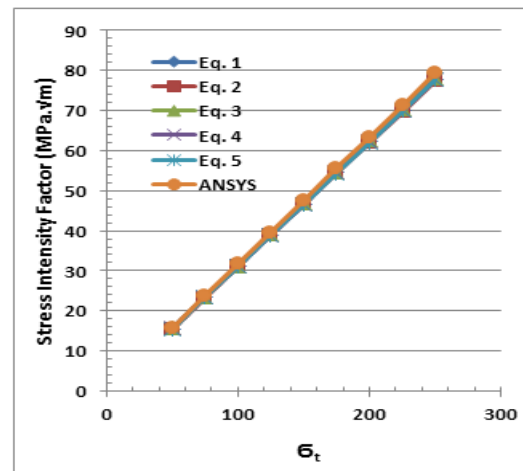


Figure 8: Variation of Stress Intensity Factor With σ_t theoretically and numerically for CCT

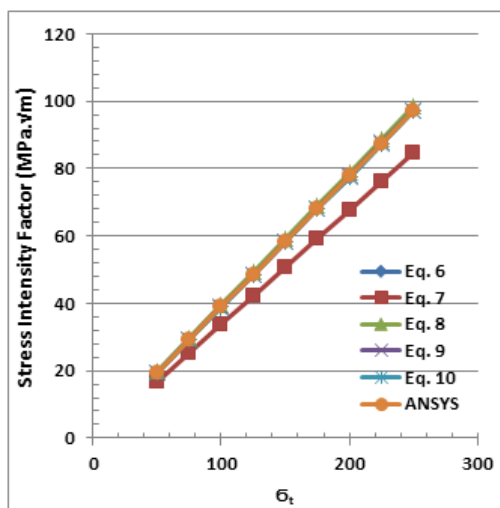


Figure 9: Variation of Stress Intensity Factor with σ_t Theoretically and Numerically for SENT

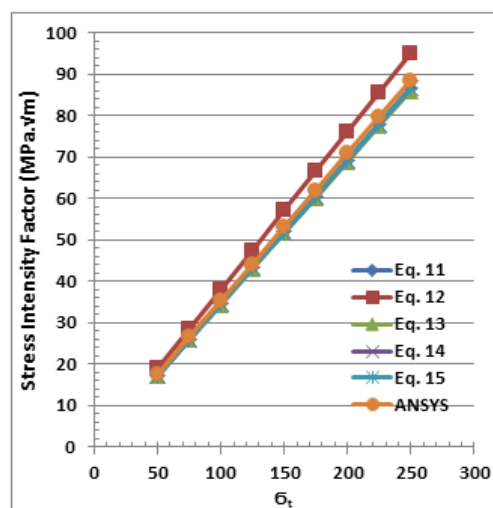


Figure 10: Variation of Stress Intensity Factor with σ_t Theoretically and Numerically for DENT

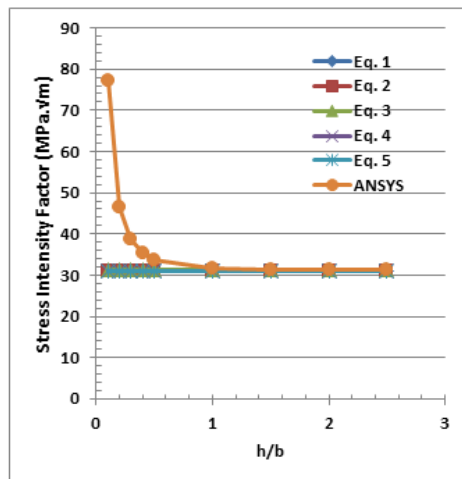


Figure 11: Variation of Stress Intensity Factor with (h/b) Ratio Theoretically and Numerically for CCT

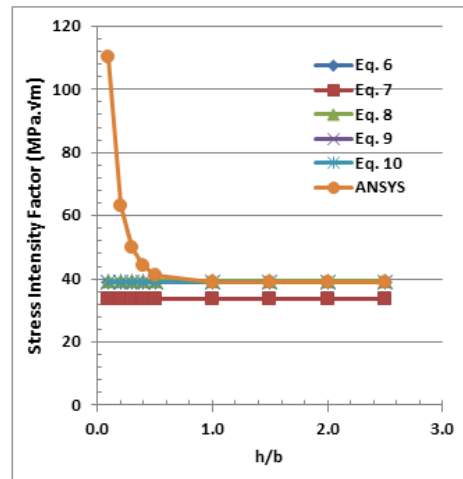


Figure 12: Variation of Stress Intensity Factor with (h/b) Ratio Theoretically and Numerically for SENT

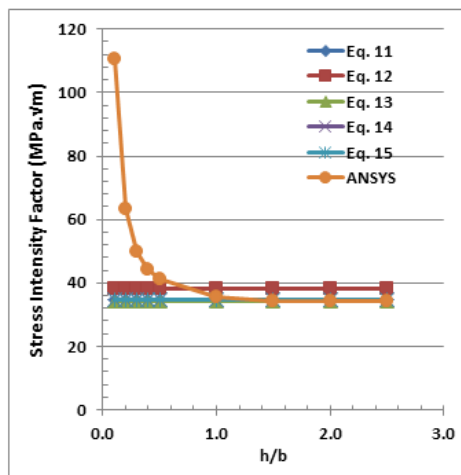


Figure 13: Variation of Stress Intensity Factor with (h/b) Ratio Theoretically and Numerically for DENT

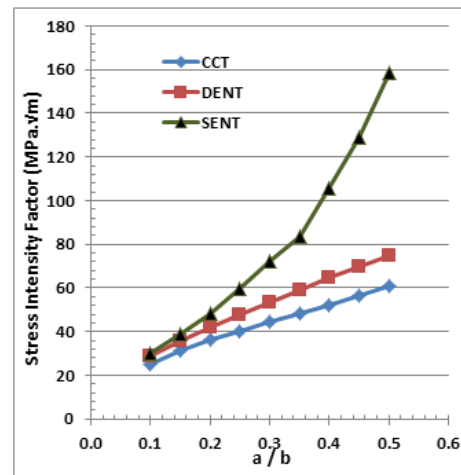


Figure 14: Variation of Stress Intensity Factor with (a/b) RATIO Numerically for CCT, SENT and DENT

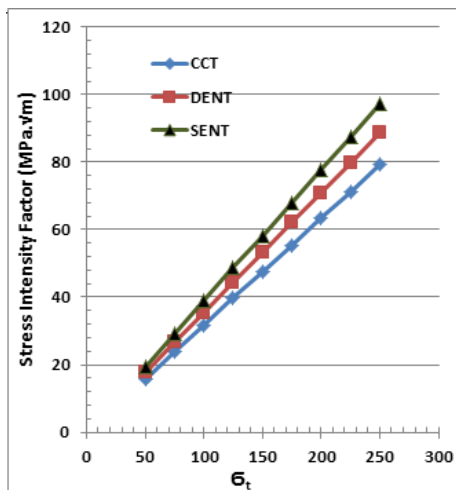


Figure 15: Variation of Stress Intensity Factor with σ_t Numerically for CCT, SENT and DENT

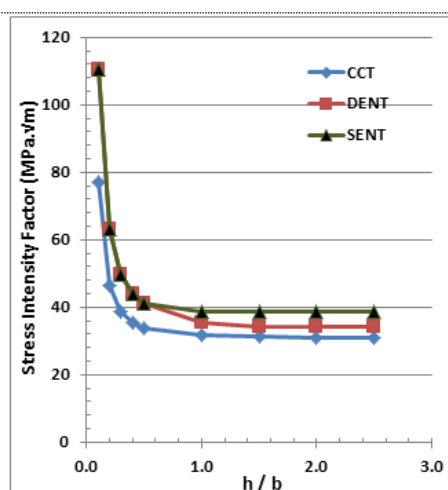


Figure 16: Variation of Stress Intensity Factor with (h/b) ratio Numerically for CCT, SENT and DENT

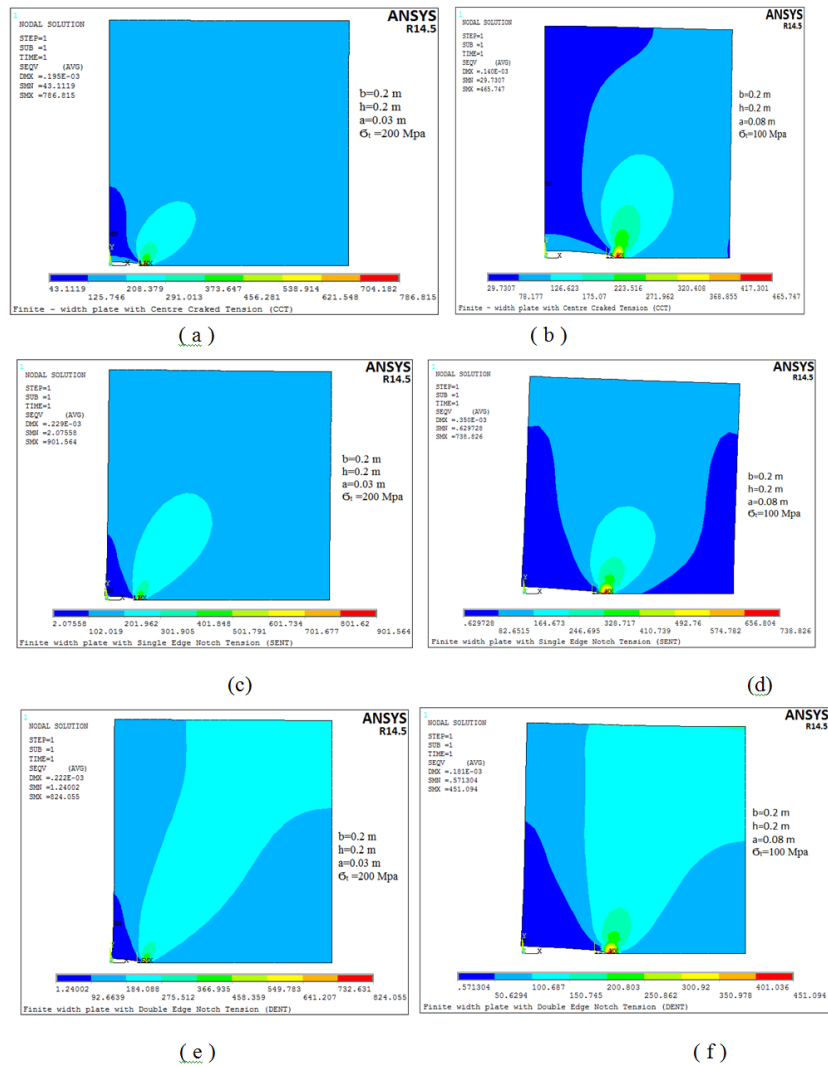


Figure 17: Von-Mises Stresses Counter Plots with Deformed Shape for 1) CCT (a & b) 2) SENT (c & d) 3) DENT (e & f)